Iranian Journal of Geophysics, Vol 20 No 6, 2027, Page 91 – 103 (Research Article)
DOI: 10.30499/ijg.2025.548140.1725

Seismic vulnerability estimation based on shear strain analysis at Mount Gamalama, Indonesia

Andri Wijaya Bidang [1*] Agustya Adi Martha [2] and Safri Burhanudin[3]

[1] *Ph.D. Student, Agency for Meteorology Climatology and Geophysics, Jakarta, Indonesia*
[2] *Ph.D., The National Research and Innovation Agency, Jakarta, Indonesia*
[3] *Associate Professor, Department of Geology, Faculty of Engineering, Hasanuddin University, South Sulawesi, Indonesia*

(Received: 20 September 2025, Accepted: 08 November 2025)

Abstract

A seismic vulnerability assessment was performed at Mount Gamalama using Horizontal to Vertical Spectral Ratio (HVSR)-derived microtremor data and shear strain estimation methods. The measurement instrument utilized was a three-component portable seismometer (Lunitek). Microtremor data acquisition was performed at 123 locations with a duration of 30-45 minutes and a spacing of 250-500 meter. The primary data consisted of recorded microtremor signals from the seismometer. within the research coordinate range of 0.7526°N – 0.868°N and 127.292°E – 127.3926489°E. Data were processed to quantify dominant frequency and amplification, which were used to model seismic responses under Peak Ground Acceleration (PGA) scenarios from 6.2%gal to 75%gal. Data processing was conducted using two platforms: Geopsy for microtremor analysis and Surfer for interpolation. Structural damage ranging from surface vibration to major cracking and collapse was identified. Zones A, B, and C were shown to exhibit increasing levels of vulnerability, with Zone A being most susceptible at high acceleration levels. Amplification effects caused by surface geological conditions were observed, particularly in zones characterized by alluvial and pyroclastic materials. Elevated shear strain values were associated with soil types D through K, reinforcing their contribution to local seismic hazard. The spatial progression of seismic risk areas was confirmed to correlate with Peak Ground Acceleration (PGA) escalation, supporting the application of this methodology for future regional disaster preparedness.

Keywords: Seismic, Gamalama, HVSR, vulnerability, microtremor

*Corresponding author: andri.wijaya@bmkg.go.id

1 Introduction

Mount Gamalama's formation has been driven by the subduction of the Molucca Sea Plate beneath the Halmahera Plate – a tectonic process that has shaped North Maluku's volcanic landscape. This persistent convergence has not only created one of Indonesia's most active stratovolcanoes but continues to fuel its hazardous activity today.

The volcanic system generated by this subduction has been systematically monitored since 1510, with sixty-six eruptions having been documented (Venzke, 2025). This well-documented chronology establishes Gamalama as a persistently high-risk volcano, with its contemporary activity posing acute threats to Ternate's densely populated coastal and slope communities. These populations remain exposed to a spectrum of subduction-derived hazards: (1) summit magmatic eruptions, (2) rainfall-triggered lahars, (3) hybrid seismic events, (4) flank collapses, (5) liquefaction during earthquakes, and (6) tsunamis from slope failures. Subsurface dynamics directly control surface hazard intensity, where local geological conditions amplify seismic waves (Ceballo et al., 2019). This is reinforced by studies from (Helaly & Ansary, 2021) and (Akkaya, 2020), which state that the synergistic interaction between high vulnerability index (K_g) and structural deficiencies exacerbates damage from seismic ground motion. However, comprehensive mapping for seismic damage estimation from earthquake ground motions remains limited. On the other hand, approximately 200,000 residents and critical infrastructure are situated within Gamalama's hazard zones. Nevertheless, no studies have specifically examined the effects of seismic vulnerability in Gamalama. This situation highlights a critical gap addressed by the present study, whose findings are expected to impact development policies and disaster mitigation in the research area.

To bridge this knowledge gap, the Horizontal-to-Vertical Spectral Ratio (HVSR) method was employed to analyze microtremor data. This technique has been validated through its consistency with one-dimensional (1-D) amplification models in low-velocity strata (Sokolov et al., 2007). Additional validation was provided by Mirzaoglu and Dykmen (2003), who demonstrated strong agreement between HVSR spectra derived from microtremor signals, earthquake records, and theoretical transfer functions from borehole data, thereby addressing concerns about potential single-method bias.

Moreover, the HVSR method has been recognized as a cost-effective approach, as it eliminates the need for artificial seismic sources while still providing reliable subsurface characterization. Its demonstrated effectiveness in complex geological terrains (Thein et al., 2014) further supports its suitability for assessing the seismic vulnerability of the Gamalama region, where varying subsurface conditions and topographic complexity present significant analytical challenges.

The vulnerability index can be derived

from microtremor measurements, a method that is easily applicable across different sites and environmental conditions. This approach allows for an efficient estimation of both soil and structural vulnerability (Nakamura, 1997). In this study, the potential earthquake-induced damage to soil and structures was assessed using the dominant frequency and amplification factors obtained from the HVSR spectra at each measurement point. These parameters were then used to estimate damage levels corresponding to earthquake scenarios of intensity IV–X on the Modified Mercalli Intensity (MMI) scale, which were subsequently converted into Peak Ground Acceleration (PGA) values (see Table 2).

The urgency of this research arises from the confirmed occurrence of simultaneous high-frequency seismic activities within both the Gamalama volcanic edifice and the underlying Halmahera slab (Hidayat et al., 2022). This interaction creates a dual-risk scenario that poses a disproportionate threat to communities residing on the volcano's slopes. Through this study, targeted mitigation strategies can be developed to enhance the resilience of these vulnerable populations around Mount Gamalama.

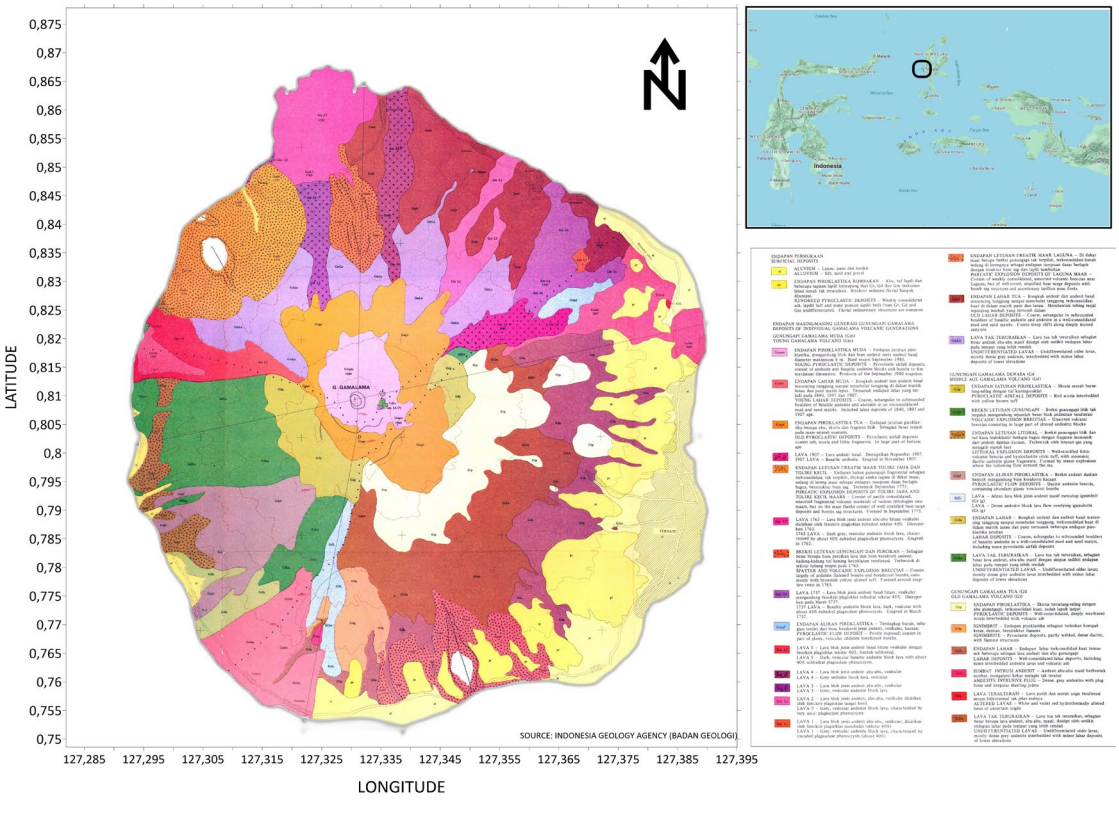

Figure 1. A geological map of Ternate Island/ Mount Gamalama, Indonesia, was presented, in which the yellow color was assigned to indicate alluvial deposits and reworked pyroclastic materials (Bronto et al., 1982).

Geology of Gamalama

Subduction beneath Halmahera is estimated to have initiated around 5 million years ago (Ma) (Hall, 1987), followed by the onset of volcanic activity approximately 3 Ma. Based on Bronto's classification, the lithological framework of Mount Gamalama comprises three volcanic generations: (1) Old Gamalama, represented by eruptive rocks distributed from the eastern to southern sectors; (2) Mature Gamalama, characterized by deposits concentrated in the southwest to west; and (3) Young Gamalama, consisting of eruptive materials extending across the west, north, and east sectors. Additionally, alluvial and reworked pyroclastic deposits—indicated in yellow on geological maps—are mainly distributed along the northeastern to southern coastal zones, with smaller accumulations present along the southwestern, western, and northwestern coasts.

2 Theory

A. HVSR (Horizontal to Vertical Spectral Ratio)

The dominant resonance frequency is determined from the peak value of the observed H/V spectral ratio, where site amplification effects are quantified through the analysis of spectral peaks. For visualization, the Geopsy software package is utilized to generate Horizontal-to-Vertical Spectral Ratio (HVSR) plots as a function of frequency. The relationship between the microtremor H/V spectral ratio at a given frequency and the respective wave motion components can be expressed using the following empirical equation:

$$H/V(f) = \sqrt{\frac{|H_{NS}(f)|^2 + |H_{EW}(f)|^2}{|V_{UD}(f)|^2}} \quad (1)$$

Where H/V is ratio horizontal component (H) and vertical component (V); $H_{NS}(f)$ and $H_{EW}(f)$ represent a fourier transform horizontal component frequencies, while $V_{UD}(f)$ denotes a Fourier transform vertical component frequency (Nakamura,1989). H/V ratio analysis confirms that the dominant resonance frequency is reliably determined from the H/V curve peak, especially when sharp. When cross-verified with earthquake data, the H/V technique is shown to consistently yield reduced amplification values, thereby delimiting its results to minimum thresholds of real amplification phenomena (SESAME).

B. Shear strain (γ)

Assuming homogeneous rock layers, the simplified equation for average shear strain (γ) is derived as follows (Nakamura, 1997):

$$\gamma = \frac{A_0 + d}{H} \quad \ldots (2)$$

Where A_0 is Amplification Factor; d is seismic displacement of the basement ground; H is surface layer thickness.

Substitute Equation (3) for basement ground acceleration (α_b) and Equation (4) for surface layer thickness (H) into Equation (2):

$$\alpha_b = (2\pi f_0)^2 . d \quad \ldots \quad (3)$$

$$H = \frac{\upsilon_b}{4A_0 . f_0} \quad \ldots (4)$$

$$\gamma = \frac{{A_0}^2}{f_0} \times \frac{\alpha_b}{\pi^2 v_b} \quad \ldots (5)$$

Where α_b is basement ground acceleration; v_b is shear wave velocity in the basement; A_0 is Amplification Factor; f_0 is dominant frequency; π is radian (3,14).

Under the assumption of uniform shear wave velocity in the basement v_b = 600 m/s, then: $1/(\pi^2\, v_b) = 1.69 \times 10^{-6}(s/cm)$, This value will be utilized in subsequent substitutions

$$\gamma = \frac{{A_0}^2 \alpha_b}{f_0} \times 1.69 \times 10^{-6} \quad \ldots (6)$$

If e =60%; $K_g(e) \cong \frac{{A_0}^2}{f_0}$ ... (7)

Where K_g = Seismic Vulnerability Index (a critical indicator for identifying high-risk soil instability sectors); e is efficiency of applied dynamic force is assumed to be e % of static force.

Ishihara (1978) established the relationship between shear strain values and ground/structure responses during earthquakes, as detailed in Table 1.

Four shear-strain regimes are defined in the table:

- $\gamma < 10^{-4}$: Elastic dominance with reversible deformation
- $10^{-4} \leq \gamma < 10^{-3}$: Micro-fracturing without progressive failure
- $10^{-3} \leq \gamma < 10^{-2}$: Elasto-plastic transition with structural macrocracking
- $\gamma \geq 10^{-2}$: Catastrophic failure modes (collapse/liquefaction/landslides).

Complementarily, ground motion-MMI correlations were established probabilistically by (Worden et al., 2012), enabling vital seismograph-to-intensity conversions (Table 2) for regional hazard assessment.

Table 1. Strain Dependence of Dynamic Properties of Soil (modified), (Nakamura, 1997).

Shear strain (γ)	Category	Soil/Building Response
$<10^{-4}$	Elastic	Soil returns to its original shape
$10^{-4} \leq \gamma < 10^{-3}$	Micro-Cracking	Not cause significant damage
$10^{-3} \leq \gamma < 10^{-2}$	Elasto-plastic	Macro cracks, potential structural damage
$\geq 10^{-2}$	Critical Failure	Liquefaction, landslide, total collapse

Table 2. Relationship Between Instrumental Intensity/Modified Mercall Intensity (MMI) Scale Peak Velocity, Peak Acceleration, Perceived Shaking, and Potential Damage (Worden et al., 2012).

PERCEIVED SHAKING	Not Felt	Weak	Light	Moderate	Strong	Very Strong	Severe	Violent	Extreme
POTENTIAL DAMAGE	none	none	none	Very light	Light	Moderate	Mod. /Heavy	Heavy	Very Heavy
PEAK ACC. (% g)	<0.05	0.3	2.8	6.2	12	22	40	75	>139
PEAK VEL. (cm/s)	<0.02	0.1	1.4	4.7	9.6	20	41	86	>178
INSTRUMENT INTENSITY	I	II-III	IV	V	VI	VII	VIII	IX	X+

C. Equipment Description and Measurement Method

Microtremor measurements were conducted using a three-component portable seismometer (Lunitek). Data were collected at 123 measurement sites, with each recording lasting 30–45 minutes and spaced approximately 250–500 meters apart. The primary dataset consisted of microtremor signals recorded by the seismometer within the research area, bounded by coordinates 0.7526°N–0.868°N and 127.292°E–127.3926°E.

3 Observation

Data processing was performed using two software platforms: Geopsy for microtremor signal analysis (Wathelet et al., 2020) and Surfer for spatial interpolation. The data processing workflow followed the SESAME Project (2004) guidelines and consisted of the following steps:

a. Application of a low-pass filter at 25 Hz,
b. Smoothing of spectral curves using the Konno–Ohmachi window function, and
c. Implementation of a window number >10 in accordance with the protocol

Shear strain values were calculated from the dominant frequency and amplification results (see Appx. A) obtained

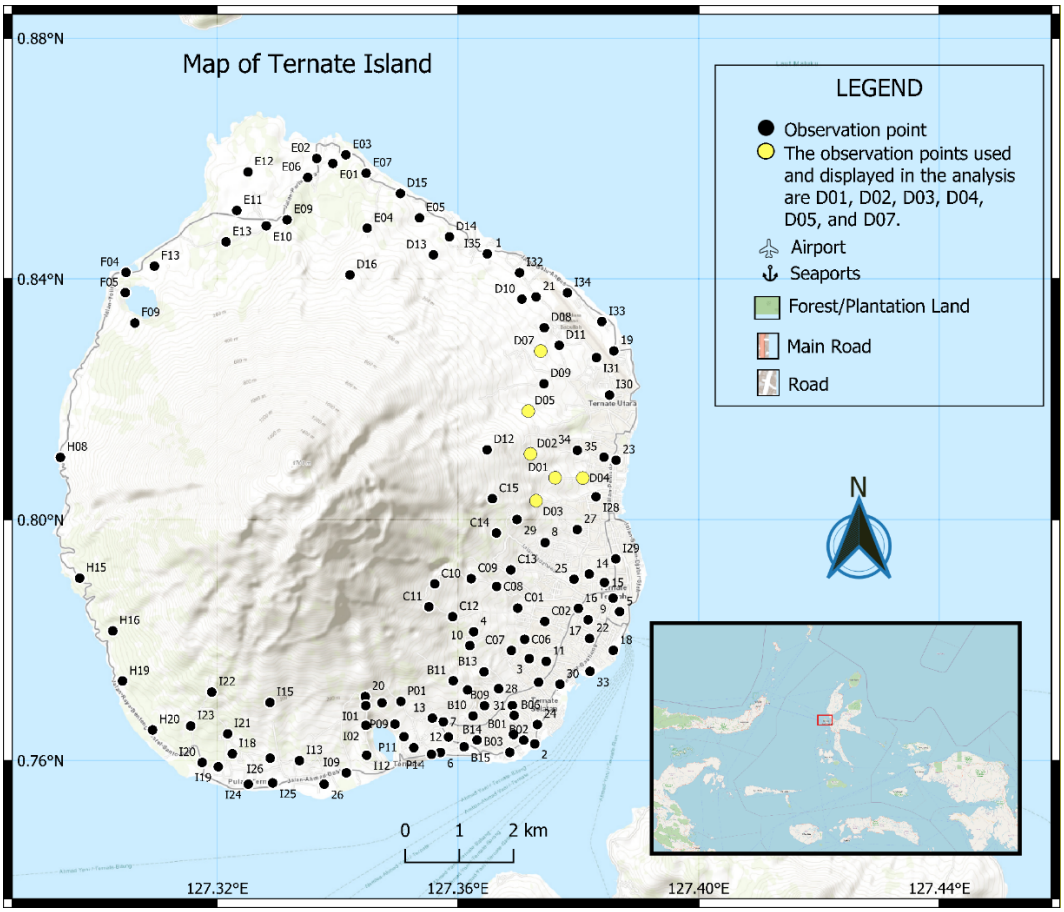

Figure 2. Study area. Black dots denote and yellow dots (D01, D02, D03, D04, D05, and D07) are Observation Points (Gamalama Volcano/Ternate City, North Maluku, Indonesia).

through microtremor HVSR data by applying various ground acceleration scenarios (according to the intensity scale in Table 2) at each measurement location. Subsequently these values were interpolated using the kriging method to construct a spatial distribution model.

The kriging method was prioritized due to its demonstrated advantages: (1) spatial structure (autocorrelation) is systematically accounted for, (2) prediction error estimates (variance) are provided, (3) flexibility with diverse data types is ensured, (4) optimal performance with sparse datasets is achieved, (5) directional variations (anisotropy) are effectively handled, and (6) applicability to complex geological scenarios is maintained (Sanchez-Brea & Bernabeu, 2005).

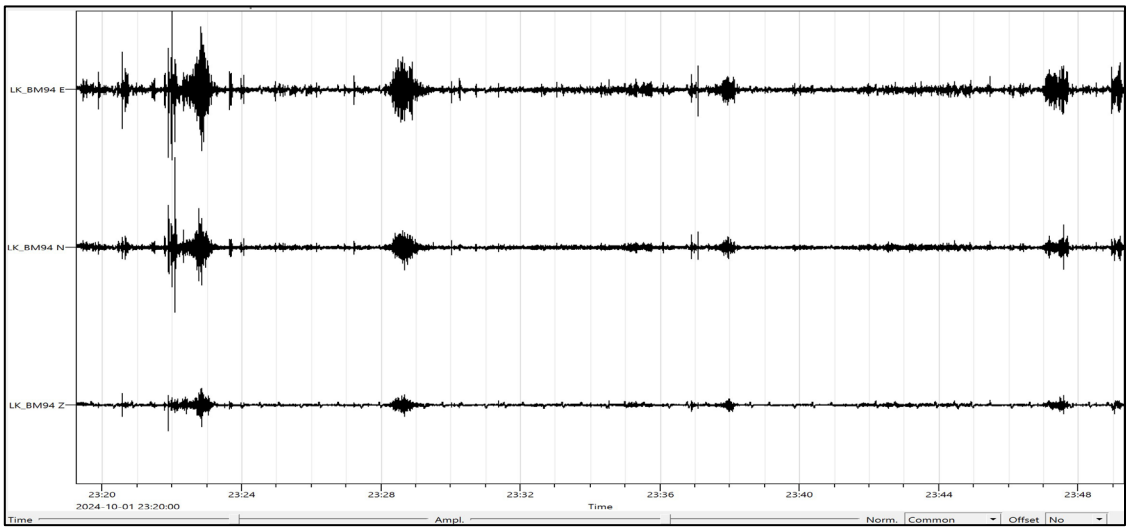

Figure 3. Microtremor signal recorded by the seismograph 3 Component (Z, N-S, E-W) at measurement point D07.

4. **Results and Discussion**

The HVSR analysis of 123 microtremor measurement points indicates that the dominant frequency ranges from 0.72 Hz to 28.642 Hz, while the H/V amplitude varies between 0.34 and 31.105.

The peak frequency was automatically identified based on the criteria established by the SESAME Project (2004), which require a single dominant peak (non-duplicated), a sufficiently pronounced amplitude (non-flat spectrum), and stability across time segments.

Challenges during data acquisition occurred mainly in densely populated or built-up areas, such as at point D01, where human activity and nearby structures may have influenced the signal quality. Nevertheless, the dominant frequency peak remained within acceptable analytical criteria. Measurements conducted under calm conditions—particularly at night—are recommended to improve data quality and signal stability.

The dominant frequency and amplification factor were subsequently used to calculate the shear strain (refer to empirical Equation (6)) under varying Peak Ground Acceleration (PGA) scenarios,

ranging from 6%g (MMI IV) to 75%g (MMI IX). The spatial distribution of the dominant damage mechanisms derived from this analysis is presented in the following table, based on the results shown in Figures 5–7.

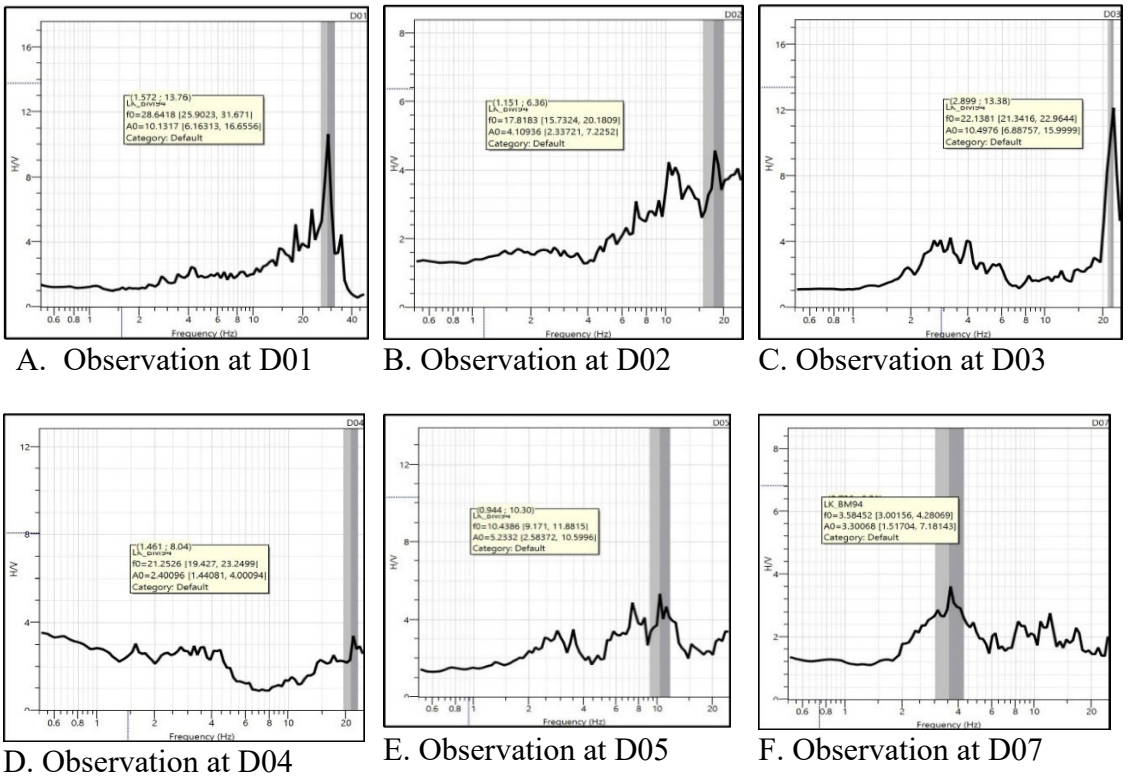

A. Observation at D01 B. Observation at D02 C. Observation at D03

D. Observation at D04 E. Observation at D05 F. Observation at D07

Figure 4. HVSR graphs at measurement points: (A) D01; (B) D02; (C) D03; (D) D04; (E) D05; and (F) D07.

At low acceleration levels (6–12%g), seismic waves propagated mainly along the surface without causing significant structural damage. Approximately 95% to 75% of the Mount Gamalama area experienced only surface vibrations, with no evidence of cracking, settlement, or repeated loading effects (see Figures 5A and 5B).

Structural vulnerability to Peak Acceleration (PA) was identified in Zone A (the Tolire Kecil phreatomagmatic maar area) and Zone B, as revealed by seismic analysis. Building damage—ranging from micro to light cracking—is expected to occur at PA levels between 6.2%g and 40%g in both zones (see Figures 5 and 6). However, when PA increases to 75%g (see Figure 7), the risk of macro-cracking and severe structural failure rises sharply, particularly in Zone A.

Numerical modeling further demonstrates a progressive expansion of microcrack-prone zones with increasing PA, indicating an intensifying seismic hazard across the region.

Zone C, which consists of volcanic deposits from the 1907 eruption of Mount Gamalama, exhibits a high potential for structural damage that increases propor-

tionally with the rise in Peak Acceleration (PA) percentage. Structures located within this zone are projected to experience micro to light cracking at PA levels between 6.2%g and 14%g (Figure 5), while substantial structural damage, characterized by the formation of large cracks, is likely to occur when PA increases to between 22%g and 75%g (Figures 6 and 7). Numerical modeling further confirms that the expansion of microcrack-affected areas grows proportionally with PA escalation, reinforcing the evidence of an increasing seismic hazard in the region. At higher acceleration levels (22–75%g), seismic waves induced the development of cracks, ground settlement, and repetitive loading effects (Figures 6 and 7), with the affected areas expanding from approximately 0.12% to 7.53%, respectively.

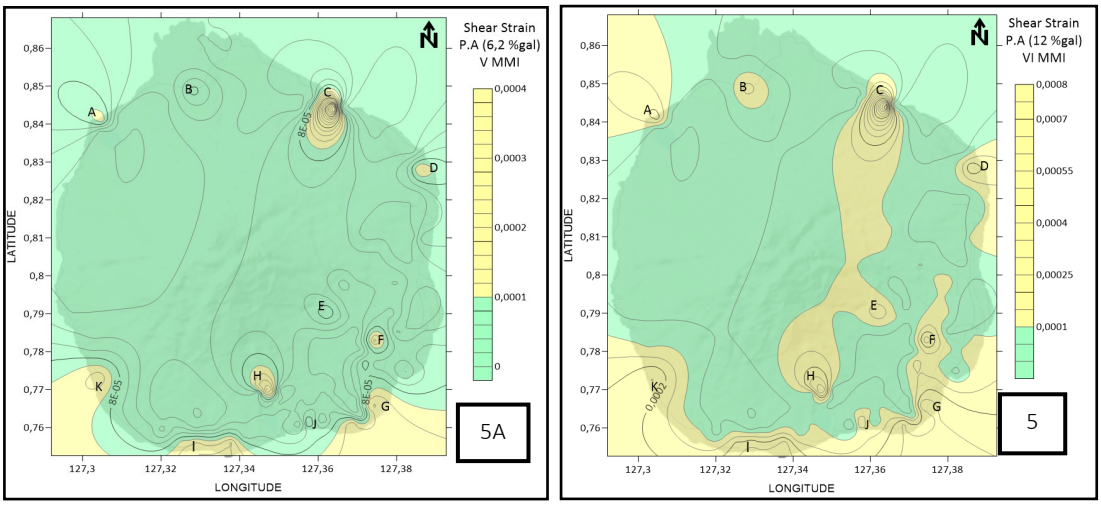

Figure 5. Seismic vulnerability maps derived from shear strain values. (A) Peak acceleration of 6.2%g associated with moderate shaking, converted to intensity level V on the Modified Mercalli Intensity (MMI) scale. (B) Peak acceleration of 12%g associated with strong shaking (Intensity level VI on the MMI scale).

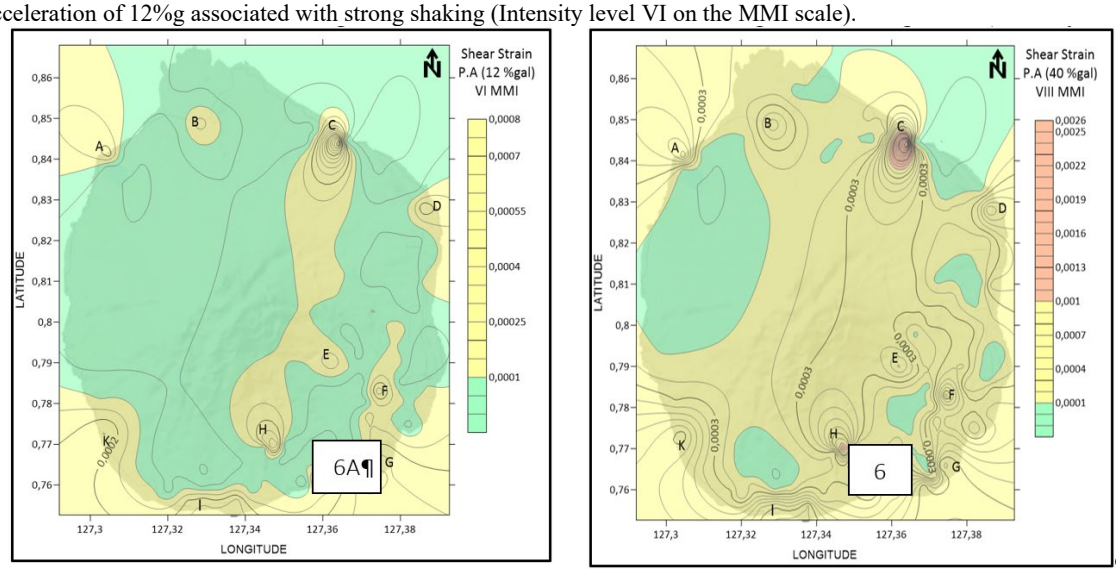

Figure 6. Seismic vulnerability maps derived from shear strain values. (A) Peak acceleration of 22%g associated with very strong shaking, converted to intensity level VII on the Modified Mercalli Intensity (MMI) scale. (B) Peak acceleration of 40%g associated with severe shaking (Intensity level VIII on the MMI scale).

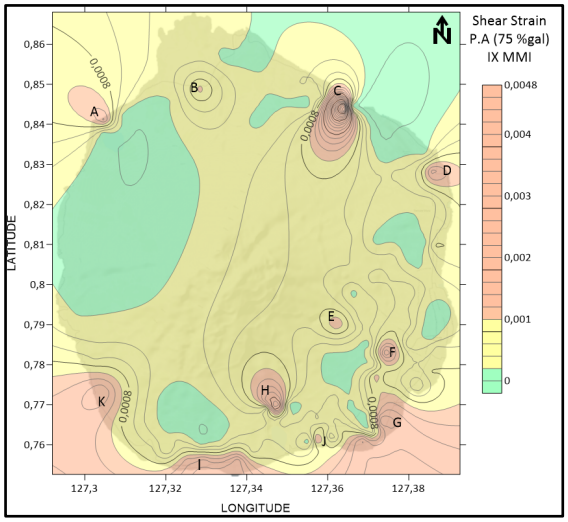

Figure 7. Seismic vulnerability maps derived from shear strain values. Peak acceleration of 75%g associated with violent shaking, converted to intensity level IX on the Modified Mercalli Intensity (MMI) scale.

Soil characteristics dominated by alluvial deposits and reworked pyroclastic materials are identified to influence seismic wave amplification and local seismic response (Clements, 1995; Lenti et al., 2009). High shear strain values, which are observed to correlate directly with increased potential seismic impact, are found primarily in regions with soil classifications D, E, F, G, H, I, J, and K. Locations A and J are among the areas that exhibit increased dominant impact with rising peak acceleration. According to Bronto et al. (1982), these locations correspond to lakes formed by phreatic eruptions, namely Tolire Lake (area A) and Ngade Lake (area J).

Table 3. The distribution of dominant damage mechanisms was identified through seismic vulnerability maps derived from shear strain values.

Scenario	Peak Acc (% gal)	Dominan Damage Category	The percentage of the area affected by Wave, Vibration (%)	The percentage of the area affected by Crack; Settlement (%)	The percentage of the area affected by Crack; Settlement/ Repeat-Speed Effect of Loading (%)
1	6,2	Vibration, very minor damage	95,44	4,56	0,00
2	12	Light to moderate cracking	74,88	25,12	0,00
3	22	Severe cracking, structural damage	43,10	56,78	0,12
4	40	Severe damage, Potential liquefaction	22,55	76,72	0,73
5	75	Widespread collapse, Potential major landslide	23,63	68,84	7,53

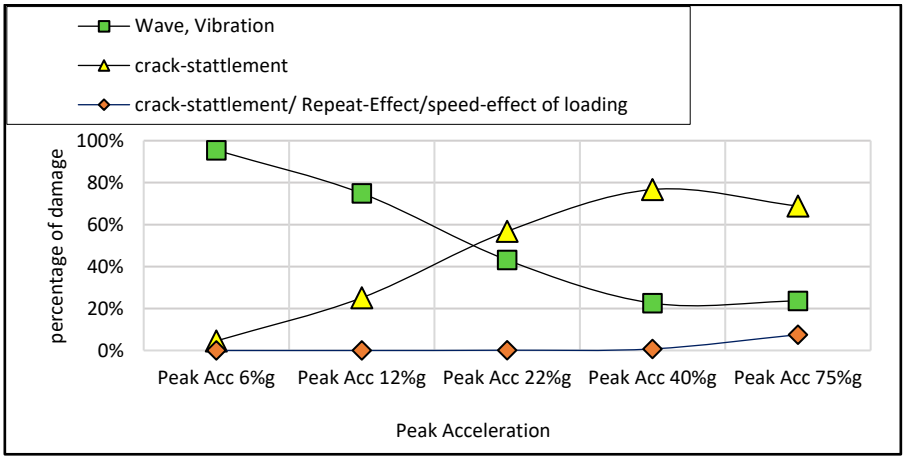

Figure 8. Graphic of the relationship between Peak Acceleration and the percentage of affected surface area.

Conclusion

a. The severity of seismic impact was found to be strongly dependent on Peak Acceleration (PA) levels. At low PA values (6–12%g), seismic activity primarily produced surface vibrations without causing structural damage. In contrast, higher PA levels (22–75%g) were associated with the emergence of cracks, ground settlements, and repetitive loading effects, accompanied by a progressive increase in the extent of affected areas.

b. Structural vulnerability to Peak Acceleration (PA) was identified across Zones A, B, and C. Zones A and B exhibit susceptibility ranging from micro to macro cracking, with Zone A showing a significantly higher likelihood of major structural failure at 75%g PA. Zone C, composed of volcanic deposits from the 1907 Mount Gamalama eruption, also demonstrates high sensitivity to PA levels. Microcracks are expected at 6.2%g–14%g PA, whereas severe structural damage is projected at 22%g–75%g PA. Numerical modeling further supports a proportional expansion of microcrack-prone areas with increasing PA, emphasizing the escalating seismic hazard within the region.

c. The local seismic response is significantly controlled by subsurface and soil characteristics. Alluvial and reworked pyroclastic materials function as amplifiers of seismic wave propagation, thereby intensifying ground motion effects. Elevated shear strain values—indicative of stronger seismic impacts—were predominantly observed in areas classified under soil types D through K Zone, suggesting their heightened susceptibility to earthquake-induced deformation

d. The increased dominant seismic impact in Areas A and J is likely influenced by Tolire and Ngade Lakes.

References

Akkaya, I. (2020). Availability of seismic vulnerability index (Kg) in the assessment of building damage in Van, Eastern Turkey. Earthquake Engineering and Engineering Vibration, 19(1), 189–204. https://doi.org/10.1007/s11803-020-0556-z

Bronto, S., Hadisantoso, R. D., & Lockwood, J. P. (1982). Peta Geologi

Gunungapi Gamalama, Ternate, Maluku Utara. Direktorat Vulkanologi.

Ceballo, R. M., González Herrera, R., Paz Tenorio, J. A., Aguilar Carboney, J. A., & Del Carpio Penagos, C. U. (2019). Effects of sediment thickness upon seismic amplification in the urban area of chiapa de corzo, Chiapas, Mexico. Earth Sciences Research Journal, 23(2), 111–117. https://doi.org/10.15446/esrj.v23n2.72623

Clements, D. L. (1995). Surface Motion of Anisotropic and Inhomogeneous Alluvial Valleys Under Incident Plane SH Waves BT - IUTAM Symposium on Anisotropy, Inhomogeneity and Nonlinearity in Solid Mechanics (D. F. Parker & A. H. England (eds.); pp. 449–454). Springer Netherlands.

Helaly, A. L., & Ansary, M. A. (2021). Assessment of seismic vulnerability index of RAJUK area in Bangladesh using microtremor observations. Soils and Rocks, 44(2), e2021057420. https://doi.org/10.28927/SR.2021.057420

Hidayat, A., Marfai, M. A., & Hadmoko, D. S. (2022). The 2015 eruption of Gamalama volcano (Ternate Island–Indonesia): precursor, crisis management, and community response. GeoJournal, 87(1), 1–20. https://doi.org/10.1007/s10708-020-10237-w

Lenti, L., Martino, S., Paciello, A., & Mugnozza, G. (2009). Evidence of Two-Dimensional Amplification Effects in an Alluvial Valley (Valnerina, Italy) from Velocimetric Records and Numerical Models. Bulletin of The Seismological Society of America - BULL SEISMOL SOC AMER, 99, 1612–1635. https://doi.org/10.1785/0120080219

Mirzaoglu, M., & Dykmen, Ü. (2003). Application of microtremors to seismic microzoning procedure. Journal of the Balkan Geophysical Society, 6(3), 143–156.

Nakamura, Y. (1997). Seismic Vulnerability Indices for Ground and Structures Using Microtremor. In World Congress on Railway Research.

Sanchez-Brea, L. M., & Bernabeu, E. (2005). Effect of noise in the estimation of magnitudes with spatial dependence: A spatial statistics technique based on kriging. AIP Conference Proceedings, 780, 811–814. https://doi.org/10.1063/1.2036872

SESAME Project. (2004). Guidelines for the implementation of the H/V spectral ratio technique on ambient vibrations: Measurements, processing, and interpretations. SESAME European Research Project. http://sesame.geopsy.org/Delivrables/Del-D23-HV_User_Guidelines.pdf

Sokolov, V. Y., Loh, C.-H., & Jean, W.-Y. (2007). Application of horizontal-to-vertical (H/V) Fourier spectral ratio for analysis of site effect on rock (NEHRP-class B) sites in Taiwan. Soil Dynamics and Earthquake Engineering, 27(4), 314–323. https://doi.org/10.1016/j.soildyn.2006.09.001

Thein, P., Pramumijoyo, S., Brotopuspito, K. S., Kiyono, J., Wilopo, W., & Setianto, A. (2014). Microtremors HVSR Correlation with Sub Surface Geology and Ground Shear Strain at Palu City, Central Sulawesi Province, Indonesia. International Journal of Innovation in Science and Mathematics, 2(5).

Venzke, E. (Compiler). (2025). Gamalama (268060) in Volcanoes of the

World (5.2.8). Smithsonian Institution. https://doi.org/10.5479/si.GVP.VOTW5-2024.5.2

Wathelet, M., Chatelain, J., Cornou, C., Giulio, G. Di, Guillier, B., Ohrnberger, M., & Savvaidis, A. (2020). Geopsy: A User-Friendly Open-Source Tool Set for Ambient Vibration Processing. Seismological Research Letters, 91(3), 1878–1889. https://doi.org/10.1785/0220190360

Worden, C. B., Gerstenberger, M. C., Rhoades, D. A., & Wald, D. J. (2012). Probabilistic Relationships between Ground-Motion Parameters and Modified Mercalli Intensity in California. Bulletin of the Seismological Society of America, 102(1), 204–221. https://doi.org/10.1769/0121111548.